energies

MDPI

Article

Usage of Ternary Gas Mixtures to Promote the Capture of Hydrogen into Hydrates: $H_2/CH_4/C_3H_8$ and $H_2/CH_4/C_2H_6$ Case Studies

Alberto Maria Gambelli [1,*], Luca Brunelli [2], Alessia Di Giuseppe [2], Fabiano Ferrari [3] and Federico Rossi [2]

[1] Civil and Environmental Engineering Department, University of Perugia, Via G. Duranti 93, 06125 Perugia, Italy
[2] Centro Interuniversitario di Ricerca sull'Inquinamento e sull'Ambiente (CIRIAF)—Interuniversity Research Center, University of Perugia, Via G. Duranti 63, 06125 Perugia, Italy; luca.brunelli@dottorandi.unipg.it (L.B.); alessia.digiuseppe@unipg.it (A.D.G.); federico.rossi@unipg.it (F.R.)
[3] Nippon Sanso Industrial S.r.l., 20159 Milan, Italy; fabiano.ferrari@nippongases.com
* Correspondence: albertomaria.gambelli@unipg.it

Abstract

Following the continuously growing demand and production of hydrogen, effective and high energy-density solutions for its storage need to be explored and validated. The present study deals with the capture of hydrogen into clathrate hydrates, at temperatures above 0 °C and relatively low pressures (<55 bar). As the formation conditions of pure hydrogen hydrates are unsuitable for industrial applications, hydrogen was firstly combined with methane, ethane and propane to form ternary gas mixtures. The role of support gases consisted in fitting both the small and the large cavities of hydrates well, thus ensuring the stability required for the hydrate lattice and allowing to hydrogen molecules to fit easily into the remaining empty cavities. Three different mixtures were selected, and the concentration of each species was defined according to the experimental results achieved in previous studies available in the literature. Chemical promoters were not used at this step, since the goal was to achieve qualitative information about the concentrations of hydrogen achievable with the proposed solution and not to maximize the volume of hydrates produced. For each species and depending on the blend of origin, the concentrations obtained in the hydrate phase were measured and reported in volume and by weight. Under the assumption of 100% cage occupancy, the quantity of each species captured in one cubic meter of hydrate, the energy corresponding to each species and the overall energy stored per unit volume of hydrate were calculated and discussed.

Keywords: gas hydrates; hydrogen storage; energy storage; ternary gas mixtures; small-chain hydrocarbons

Check for updates

Academic Editors: Bartłomiej Igliński and Michał Bernard Pietrzak

Received: 22 May 2026
Revised: 19 June 2026
Accepted: 22 June 2026
Published: 24 June 2026

Copyright: © 2026 by the authors. Licensee MDPI, Basel, Switzerland. This article is an open access article distributed under the terms and conditions of the Creative Commons Attribution (CC BY) license.

1. Introduction

Gas hydrates are non-stoichiometric crystalline structures composed of hydrogen-bonded water molecules (guests) forming polyhedral cavities including gaseous molecules (hosts) [1]. The formation of hydrates is also possible at thermodynamic conditions unfeasible for the formation of ice, therefore representing a possibility for water molecules to reach a more ordered and stable configuration at given pressure and temperature conditions [2]. The presence of gas molecules is required to avoid the collapse of water cages, while the presence of adjacent cages avoids possible dissociation due to opposite forces.

Gas molecules are physically but not chemically trapped within the solid lattice: only van der Waals forces exist between gas and water molecules, and the energy required to break van der Waals bonds is equal to 1.25 kJ/mol, significantly lower than the corresponding quantity for hydrogen bonds (approximately 20.92 kJ/mol) [3]. In general, gas hydrates require relatively high pressures and low temperatures to be formed [4], and the specific conditions strictly depend on the typology of guest species included in the crystalline structure [5]. Several gases are capable of forming hydrates, and their main common property is hydrophobicity, even if some exceptions are worthy of being mentioned, such as carbon dioxide and hydrogen [6]. Among them, the most relevant species are methane and, more generally, small-chain hydrocarbons, carbon dioxide, some noble gases, as xenon and krypton, oxygen, nitrogen, hydrogen sulfide and hydrogen [7–10]. The size and geometry of gas molecules are crucial parameters governing hydrate formation: gas species must be small enough to enter the cavities but, at the same time, sufficiently large to completely fit those cavities, thus providing them the required stability [11]. Water molecules are hydrogen-bonded to each other also in the liquid phase; the difference in terms of number of hydrogen bonds between the liquid and the solid phase is approximately equal to 15%. In the liquid phase, hydrogen-bonded water molecules commonly form polygonal faces such as, in order of probability, pentamers, hexamers and squares. That probability is a function of the internal angles of the polygons. Due to the electronegativity of oxygen, the bond angle of water is 104.5°, slightly lower than 109.5°, or the angle of a perfect tetrahedron. Pentamers are the most diffused solutions for hydrogen-bonded water molecules, as the internal angle of these figures is 108°. Pentamers are then followed by hexamers and squares. Heptagons and octagons are also possible, although the probability of their existence is much lower. The typology of connections between water molecules in the liquid phase strongly affects the size and geometry of the cavities forming hydrates. Five different cavities exist in nature and are defined using the nomenclature "ni^{mi}", where "ni" is the number of edges of the "i" face, while "mi" is the number of faces exhibiting "ni" edges [12]. According to the present nomenclature, the five possible polyhedral cages are defined as follows: pentagonal dodecahedron (5^{12}), tetrakaidecahedron ($5^{12}6^2$), hexakaidecahedron ($5^{12}6^4$), irregular dodecahedron ($4^35^66^3$) and icosahedron ($5^{12}6^8$) [13]. The aggregation of these cavities leads to the formation of three hydrate structures: cubic sI [14], cubic sII [15] and hexagonal sH [16].

The main reason for scientific and industrial interest in gas hydrates can be attributed to the huge quantity of methane reserves they constitute worldwide. According to the current estimations, the quantity of methane included in natural gas hydrate reservoirs is enough to produce twice the energy still achievable by consuming all the conventional fossil energy sources (oil, natural gas and coal) currently available [17]. In addition, hydrates compounds are gaining growing interest for the peculiar properties of their formation and dissociation properties, together with their capability of capturing high quantities of gas in a relatively contained volume [18]. According to this, the formation and melting processes could be advantageously applied for the capture and final disposal of CO_2 [19,20] and, similarly, for the storage and transportation of energy gases [21,22]. Moreover, hydrates can also be exploited for cold energy storage [23], desalination [24], removal of contaminants from wastewater [25], food concentration [26,27] and other applications.

The storage of energy gases in hydrate form is gaining growing scientific and industrial interest, because of the possibility of storing gas in solid form at much lower pressures than cylinders, thus ensuring easier and safer transportation. Methane hydrates represent a competitive alternative to liquid methane, since pressures lower than 50 atm and temperatures above 0 °C are sufficient for their formation while, considering the same pressures, temperatures equal to −83 °C are required for methane liquefaction [28]. The production of

hydrates for energy gas storage is also attractive because of the high energy density, which can be theoretically reached (comparable to pressurized cylinders).

Unlike methane, the production of hydrogen hydrates is more complex and requires excessive pressures to occur: at room temperature, more than 20,000 bar are required to produce pure hydrogen hydrates [22]. The most widespread solutions for hydrogen storage are pressurized cylinders [29], cryogenic technologies [30], the use of porous materials [31] and metal hydrides [32]. Unfortunately, each solution mentioned presents critical issues. The storage into pressurized vessels requires pressures ranging from 35 to 70 MPa, with the related consumption of energy for the pressurization phase. In addition to this, vessels suitable to host hydrogen are, on average, more expensive [33]. Cryogenic applications avoid the need of dedicated vessels; on the other side, the liquefaction of hydrogen is possible exclusively at extremely low temperatures (−253 °C or lower), with consequent uncompetitive energy costs [34]. Regarding the remaining options, the availability and cost of raw materials represent the main limiting factor to their diffusion [35].

In general, the low density of hydrogen (0.089 kg/m^3) remains one of the main barriers to overcome.

Hydrogen storage in hydrate form was firstly proposed during the 1990s [21]. To reduce the unacceptable pressures required for the process, a wide variety of thermodynamic and kinetic chemical additives was proposed and tested [36,37]. The usage of chemical additives still introduces further variables, related to their availability, environmental availability, safety for humans and costs. An alternative option consists of producing hydrates with H_2-containing mixtures instead of pure hydrogen [38]. The introduction of support gases, whose size is suitable for fitting and stabilizing the cavities of the hydrate lattice, is capable of reducing the formation pressure about one order of magnitude or more. Among the various approaches proposed in the literature, the use of mixed-gas hydrate systems represents a promising solution for reducing hydrate formation pressures while maintaining significant hydrogen storage capacities. For this reason, the present work focuses on the use of ternary mixtures containing hydrogen and selected hydrocarbon support gases.

Following the latter proposal, this study investigates the capture and storage of hydrogen into hydrates by using small-chain hydrocarbons (methane, ethane and propane) as support gases. Ternary mixtures were thought for the scope: hydrogen and two species to stabilize, respectively, the small and the large cages. The first step, carried out in previous studies, consisted of selecting the support gases and evaluating their capability to operate together and create synergy. The results are briefly resumed in the following paragraph of this manuscript. In the experimental section, the selected mixtures where combined with hydrogen at different concentrations and used for hydrates formation. The gas phase captured into hydrates was finally analyzed to define the quantity of hydrogen which can be theoretically captured in the unit volume of hydrates.

2. Support Mixtures for H_2 Storage and Role of Each Species Involved

The role of guest molecules substantially consists of fitting the water cages, thus preventing their collapse and ensuring the stability of the crystalline lattice. Guest species must have a molecular diameter lower than the cavity diameter but, at the same time, the difference between the two values must be relatively small to ensure the correct filling of cages. However, in the case of excessively small difference, the geometry of guest molecules becomes crucial. The size of the hydrogen molecule does not allow the stabilization of any of the cavities forming hydrates. Therefore, the production of hydrates, with pure H_2 as the guest, requires extremely high pressures to compensate for the different size between cages and guest molecules. Based on these considerations, the selection of suitable support gases becomes a key aspect of the development of hydrate-based hydrogen storage systems

operating under moderate pressure conditions. The identification of species capable of stabilizing both small and large hydrate cavities is therefore essential to enhance hydrogen incorporation while reducing formation pressures.

Based on the gas species used as support gases the formation of sI and sII hydrates was considered. Both structures include large ($5^{12}6^2$ in sI and $5^{12}6^4$ in sII) and small (5^{12} in both structures, even with a little difference in terms of cavity diameter) cavities. The size of those cavities suggested the need for two support gases, to use together, to stabilize the hydrate lattice, since hydrogen cannot stabilize any cavity (at the P-T conditions considered in this study) and can exclusively fit into the vacant empty cavities.

The first mixture tested included CO_2 and C_3H_8 and was studied in Gambelli (2024) [39]. Carbon dioxide was selected to explore the possibility of reusing a greenhouse gas, instead of releasing it into the atmosphere. Conversely, propane was chosen for its capability to form hydrates at extremely low pressures, when the local temperature is kept below (approximately) 5.5 °C. In contrast with the latter observation, the addition of propane, even if at low concentrations, did not promote the formation of hydrates and even produced an opposite effect. Carbon dioxide spontaneously forms sI hydrates, mainly occupying the large cavities; similarly, propane molecules form sII hydrates and fit into the large cavities. While carbon dioxide can easily enter into the large $5^{12}6^4$ cages of sII, the molecule of propane cannot enter the $5^{12}6^2$ cages. Therefore, the inclusion of both guest species in the same hydrate cell is unlikely, since the two gases would compete with each other to occupy the same cavity. For that reason, the two species formed hydrates separately and no promoting action was possible. Conversely, the addition of propane, even if at low concentrations, reduced the partial pressure of CO_2 in the gas mixture and the formation curve consequently shifted to higher pressures. A similar trend was also observed in tests carried out with CO_2/C_2H_6 mixtures [40]. By itself, ethane produces sI hydrates, exclusively fitting the large $5^{12}6^2$ cavities (the cage filling ratio is higher than the one for the smaller cavities, which remain empty). Therefore, ethane and carbon dioxide molecules would compete to occupy the same cavity in the same structure. This study confirmed this, showing that the overall forming conditions approximately remained those of pure CO_2 hydrates, or even more severe, while the melting conditions showed an intermediate trend between the phase equilibrium of hydrates produced with the two species separately [40]. Two further aspects are worthy of mentioning. First, the P-T conditions substantially changed as a function of the more abundant guest species present in the gas mixture. Even with a certain deviation, due to the competition between the two gases, the system mainly followed the trend of the most abundant species (when used in pure form). It means that, when a CO_2/C_2H_6 (75/25 vol%) mixture was used, the forming and melting conditions were more severe (closer to those for pure CO_2 hydrates) than those observed with the CO_2/C_2H_6 (25/75 vol%) mixture since, in general, ethane requires milder thermodynamic conditions to be captured into hydrates. The second aspect to mention is the lower contrast observed between the two species, if compared with the CO_2/C_3H_8 mixtures previously described. This latter aspect can also be explained in terms of cage occupancy. Propane molecules can be captured exclusively within sII hydrates, and carbon dioxide cannot fit into the small 5^{12} cavities in this structure. Conversely, it is possible, even if unlikely, for CO_2 molecules to fit into the small 5^{12} cages in sI, making the formation of a tiny quantity of mixed hydrates possible.

The same two hydrocarbons were then tested with methane instead of carbon dioxide. In this case, the rationale was twofold. Methane molecules can easily fit into the small cavities of both sI and sII hydrates; moreover, the final separation (before usage) of support gases from hydrogen is necessarily required, since CH_4/H_2 mixtures, under appropriate concentrations, can directly replace natural gas in a great number of applications, without

the need to modify infrastructures and with benefits in terms of power produced, reduced pollution and ignition properties [41,42]. The use of methane in mixture with propane was tested in [39]. The experiments proved that the two species were simultaneously captured in the same cells, thus forming hydrates at pressure–temperature conditions much milder than those describing the formation of pure methane hydrates. In this case, sII hydrates were formed, since propane molecules cannot be captured in sI (at the P-T conditions selected for this study). Propane molecules occupied the large $5^{12}6^4$ cavities, while methane molecules occupied the small 5^{12} cages. Such a configuration provided great stability to the system: the cage filling ratio for propane in 16-hedra cavities is equal to 0.943 and that for methane in the 12-hedra cavities is 0.868 (higher than the same value for sI, equal to 0.855). The dissociation curves confirmed the high stability of the system: hydrates dissociated at temperatures much higher than those causing the melting of pure methane and pure propane hydrates. That binary mixture probably represented the most favorable option for gas storage, compared with the other systems discussed in this section, since it promoted the formation of hydrates and ensured their stability, thus making the further steps (storage and transportation) easier.

A good level of synergy was also observed between methane and ethane [43]. The two gases cooperated in forming the same hydrate cells, with an overall promoting effect observed both during the formation step, which occurred at lower pressures and/or higher temperatures, and during the final dissociation, which was widely shifted to higher temperatures, if compared with the phase equilibrium conditions of the two respective species. The CH_4/C_2H_6 mixtures led to the production of sI hydrates, where the two species respectively fit and stabilize the small and large cavities. These findings provided the rationale for selecting methane/propane and methane/ethane systems as support mixtures for the hydrogen storage experiments discussed in the following sections.

3. State of the Art on Hydrogen-Containing Hydrates

In addition to the studies discussed in the previous section on hydrate-forming support gases, it is important to review the current state of the art concerning hydrogen-containing hydrate systems and their potential applications.

In the literature, the application of gas hydrates in the field of hydrogen storage has gained increasing attention in recent years. Hydrogen hydrates are of particular interest due to their potential advantages, such as moderate storage pressures compared to compressed gas systems, intrinsic safety and the possibility of tuning storage capacity through the use of promoters and mixed-gas systems. These characteristics make hydrate-based storage an appealing option for stationary applications, seasonal energy storage and the integration of hydrogen with renewable energy sources [44].

Lim et al. [45] classified gas hydrates as solid-state materials offering several advantages due to their high storage capacity. Englezos et al. [46] stated that, thanks to their high gas storage capacity, gas hydrates can offer opportunities for the development of innovative technologies, such as the separation of CO_2 from CO_2/N_2 and CO_2/H_2 mixtures, CO_2 sequestration, natural gas transportation and storage and H_2 storage. The main difficulty in forming hydrogen hydrates remains the high pressure required for their formation. Therefore, Lang et al. [47] proposed the use of tetrahydrofuran (THF), tetrabutylammonium bromide (TBAB) and tetrabutylammonium fluoride (TBAF) to significantly decrease the hydrogen hydrate formation pressure. Rothmund et al. [48], using molecular dynamics simulations, investigated a two-level promotion strategy for effective hydrogen storage under mild conditions (e.g., 260 K and 100 bar), combining methane (CH_4) as a thermodynamic promoter and nanoporous activated carbon as a host material to exploit the beneficial effects of confinement. Another role of hydrogen in the field of gas hydrates

is as a promoter in replacement processes. CO_2 replacement is considered particularly attractive because it enables the simultaneous production of hydrate-bound natural gas and the sequestration of CO_2 [49]. Chaturvedi et al. [50] demonstrated the feasibility of injecting mixed flue gas compositions (CO_2 + N_2) together with low concentrations of H_2 as a diluent to recover CH_4 from natural gas hydrate reservoirs.

Sun et al. [51] proposed a semi-continuous CO_2/H_2 injection–production mode, in which the continuous injection–production process is periodically interrupted by stopping injection and production operations to allow sufficient diffusion of the injected gas, thereby improving CH_4 recovery and CO_2 storage.

In addition, Sun et al. [52] conducted a series of experiments to optimize the composition and flow rate of the injected gas, which have a significant effect on the decomposition rate of CH_4 hydrate, the amount of CO_2 sequestration and the overall cost, thereby establishing a balance between CH_4 production and CO_2 sequestration. Wang et al. [53] also observed that the composition of CO_2 and H_2 in the feed gas significantly affects both gas production and CO_2 sequestration. An increase in the molar fraction of H_2 leads to a higher cumulative gas production ratio during the gas sweeping and replacement phases but reduces the CO_2 sequestration ratio, defined as the amount of CO_2 captured by the hydrate relative to the total CO_2 injected into the hydrate layer. Conversely, increasing the molar fraction of CO_2 in the feed gas results in a higher CO_2 sequestration ratio but reduces both the gas production rate and the cumulative methane production ratio. Overall, the available literature confirms the potential of hydrate-based systems for hydrogen storage, while also highlighting the need for alternative solutions capable of reducing formation pressures without relying exclusively on chemical promoters. In this context, the use of ternary mixtures containing hydrogen and hydrocarbon support gases represents a promising research direction and constitutes the focus of the present work.

4. Materials and Methods

The reactor used to carry out the experiments is described in Section 4.1, while the experimental procedure and materials used for the experiments are respectively discussed in Sections 4.2 and 4.3.

4.1. Experimental Apparatus

The experiments were conducted in a small-scale pressure reactor designed to carry out hydrate formation and dissociation processes under laboratory conditions. The reactor (model RC-PED-DN80-100B-GS, Metalserbatoi, Torgiano (PG), Italy), constructed entirely of AISI 304 stainless steel, has a cylindrical geometry with 15 mm thick flanged flat ends. It features a useful internal length of 350 mm, an internal diameter of 88.9 mm (DN80) and a total internal volume of 2173 cm^3 (approximately 2.2 L) (Figure 1).

The reactor is oriented horizontally to increase the gas–liquid contact surface area. Mechanical support is provided by two brackets welded to the reactor body, which are bolted to a pickled carbon steel trolley.

The internal volume can be accessed through a 32 mm thick flange with an external diameter of 230 mm, located on the lower flat end. The sealing is ensured by a spiral-wound metal gasket (model 316L/FG DN80PN100) positioned between the mating flanges.

For continuous visual monitoring during the experimental tests, two sight glasses are installed at mid-height along the cylindrical body, allowing direct observation of the interior during operation without opening the vessel.

The reactor is equipped with multiple threaded connections distributed along the external jacket. In the lower section of the shell, a 1/2″ drain valve allows controlled discharge of residual contents and accumulated fluids from the pressure vessel.



Figure 1. Image of the assembled reactor.

The upper section of the shell includes:

- One 1″ sand inlet connection;
- One 1/4″ gas inlet connection;
- One 1/4″ gas outlet connection;
- A safety valve;
- A digital pressure gauge.

Water is introduced through the sand inlet connection due to its larger diameter. Gas is injected from the top of the reactor rather than from the bottom to prevent liquid water from flowing back into the gas supply line under gravitational effects. Such backflow could reduce the effective internal volume available for hydrate formation and potentially cause blockages or malfunctions in the gas injection system.

The gases are introduced through two separate lines made of copper tubing, designed to deliver the different gases used in the experiments.

The gas lines are connected by a T-fitting, downstream of which a stainless steel needle valve (model H99S10SSRV1/4, HAM-LET Group, Nazareth, Israel) is installed to regulate and shut off the incoming gas flow. Rapid depressurization of the gas phase is achieved by opening the main needle shut-off valve (model H99S10SSRV1/4, HAM-LET Group, Israel), located at the top of the reactor. Upstream of this valve, a fine flow-control valve (model FT2251, Tognella S.p.A., Somma Lombardo (VA), Italy) is installed to allow controlled gas sampling for subsequent gas chromatography analysis.

To protect the system from overpressure, an automatic safety valve (model E10/LS, Nuova General Instruments, Pianello Val Tidone (PC), Italy) is mounted directly on the reactor body. The valve is set to a calibration pressure of 80 bar, ensuring an adequate safety margin.

Local pressure is monitored using a digital pressure gauge (model MAN-LD3S5C2S, Kobold Instruments, Settimo Milanese (MI), Italy) with an accuracy of ±0.5% of full scale.

The internal temperature is measured by two Type K thermocouples (Class 1 accuracy; measurement uncertainty ±0.1 °C). The sensors are mounted on the cylindrical wall of the reactor at two different heights: T01 (length 10 cm), immersed in the liquid phase, and T02 (length 20 cm), positioned in the gas phase. This configuration provides a more

representative and reliable assessment of the thermal behavior of the system and was designed according to previous studies carried out in vertical-axis apparatuses [54,55].

All sensors are connected to a Seneca data acquisition system (model Z-8TC-SI LAB, Padua, Italy).

Temperature control is achieved by placing the reactor inside a 3 × 3 × 3 m cooling chamber, capable of maintaining the internal temperature with an accuracy of ±0.1 °C.

A photograph and a schematic diagram of the experimental apparatus are shown in Figure 2.

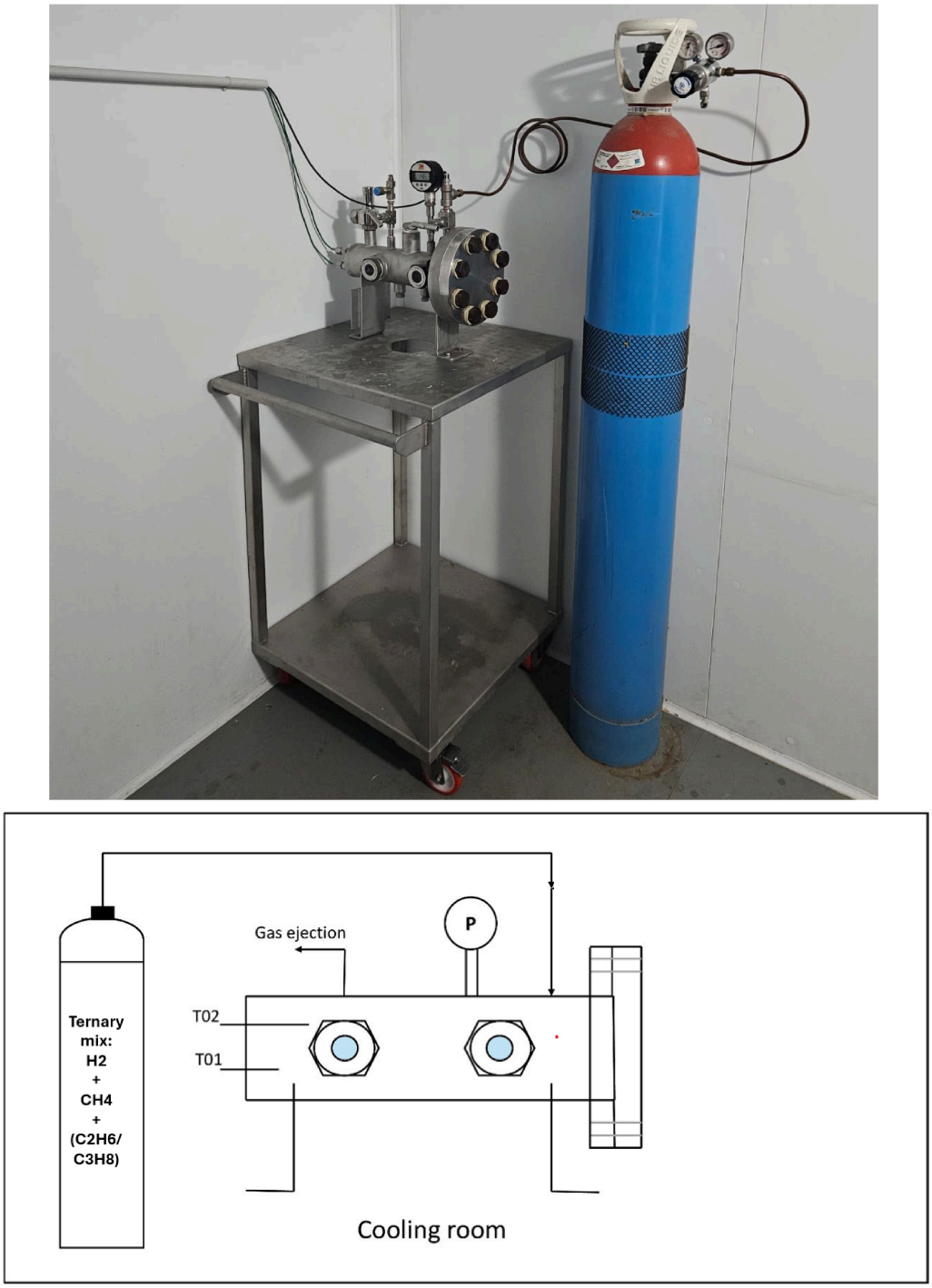


Figure 2. Image and schematic diagram of the experimental apparatus.

The gas sample was collected using a pressurized sampling cylinder (manufactured by Metalserbatoi, Torgiano (PG), Italy) with an internal volume of approximately 120 cm^3. The cylinder body is made of stainless steel, a material suitable for hydrogen containment, thereby preserving sample integrity.

The system is equipped with a manual shut-off valve located at the top, which enables flow control during sampling and ensures proper isolation of the collected sample. An analog pressure gauge mounted on the side allows continuous monitoring of the internal pressure, ensuring safe operating conditions during sampling and subsequent handling (Figure 3).



Figure 3. Image of the cylinder used for gas samplings.

Prior to each sampling procedure, the internal volume of the cylinder was purged with an inert gas, consisting of a species different from those involved in the production of hydrates. In this work, nitrogen was used for that scope.

4.2. Experimental Procedure

Experiments were carried out to understand the promoting effect of support gases for the capture of hydrogen into hydrates. Therefore, the procedure followed for hydrate formation and melting was not focused on maximizing hydrates production or defining the phase equilibrium of the system. Consequently, chemical promoters were not considered at this step. In addition, experiments were carried out in excess of gas to ensure the best conditions possible (at fixed initial pressure and temperature) for the capture of gas molecules. Experiments carried out in excess of water allow guest molecules to be captured until pressure stabilizes, thus defining the phase boundary equilibrium conditions for the system [56], which were not the focus of this study.

The formation step started at high pressure, ranging from 52 to 55 bar, and at temperatures high enough to ensure the initial absence of hydrates and to prevent the occurrence of the memory effect in the system [57,58]. Therefore, each test started at room temperature (higher than 20 °C) or, considering the initial pressures used, widely outside the hydrate-formation region. In detail, 0.4 L of water was inserted into the reactor and, depending on the initial pressure, approximately 3.8–4.0 moles of gas were injected into the reactor. This means that the initial gas–water ratio ranged from 5.8 to 5.6, denoting an initial excess of gas within the reactor.

For gas injection, the reactor was directly connected to the gas cylinder, and both devices were positioned within the cooling room, to prevent internal gradients of temperature due to gas flow (see Figure 4).

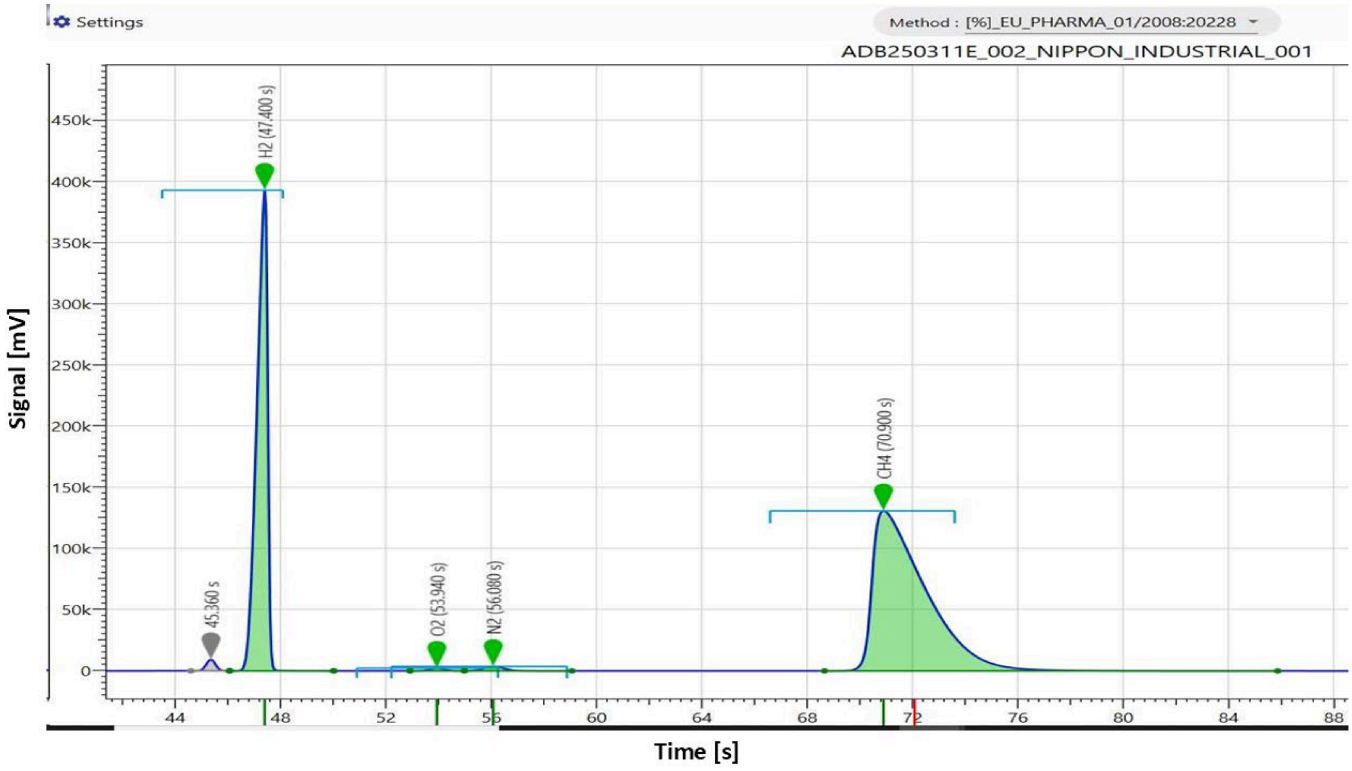


Figure 4. Chromatogram describing the composition of the gas mixtures captured into hydrates, when Mixture 1 was used for the process.

The cooling room was them switched on and the internal temperature gradually reduced, until approaching the freezing point of water (from the room temperature until approaching 0 °C; cooling rate approximately equal to 0.6–0.9 °C/h). In addition to the natural reduction, associated to the decrease of temperature, the internal pressure also decreased as a consequence of the process evolution: the capture of gas molecules within crystalline water cages, reduced the presence of guest molecules in the gas phase, with a consequent lower pressure. The process was prolonged over time, to produce enough hydrates for gas samplings, then used to detect the presence of hydrogen within the crystalline lattice.

After completing the production step, the gaseous phase remained in the reactor and was quickly ejected, leaving exclusively the hydrate phase inside the reactor. This latter operation was carried out without pre-subcooling the system; therefore, part of the formed hydrates melted and the mixture contained in them escaped from the reactor. As previously stated, these experiments were not designed to define the quantity of hydrates produced but aimed exclusively at detecting the gas composition achievable within hydrates, with particular attention to the hydrogen content.

After gas ejection, the reactor was closed again and the melting of hydrates took place. The vessel shown in Figure 3 was then attached to the ejection channel and gas samples were collected. The chromatographic analysis was performed using a Varian CP-4900 Micro GC (by Agilent Technologies, Santa Clara, CA, USA) gas chromatograph equipped with a TCD detector and Molsieve 5A and PoraPLOT Q columns, with Ar as the carrier gas and a detection threshold for hydrocarbons of 10 ppm.

4.3. Materials

For the experiments discussed in this study, pure demineralized water was used. The gas mixtures are listed in the next section and were provided by Nippon Gases SrL (Milano, Italy) and have purity degree equal to 99.99%.

5. Results and Discussion

Based on the main findings highlighted in Section 2, three hydrogen-containing mixtures were considered in this study. As previously specified, carbon dioxide was not considered, due to the lack of any synergistic effect when mixed with propane and ethane. Two of the selected mixtures contain methane and propane, while the third mixture is formed by methane and ethane.

The three mixtures used in this study are summarized in Table 1.

Table 1. Composition of the ternary gaseous mixtures used to form hydrates.

Mixture 1		Mixture 2		Mixture 3	
H_2	30.00 ± 0.01 [vol%]	H_2	40.00 ± 0.01 [vol%]	H_2	30.00 ± 0.01 [vol%]
CH_4	60.00 ± 0.01 [vol%]	CH_4	50.00 ± 0.01 [vol%]	CH_4	52.00 ± 0.01 [vol%]
C_3H_8	10.00 ± 0.01 [vol%]	C_3H_8	10.00 ± 0.01 [vol%]	C_2H_6	18.00 ± 0.01 [vol%]

Regarding the mixtures containing propane, the concentration of this latter species was defined according to the results described in Gambelli A.M. (2024) [39]. The addition of 10 vol% C_3H_8 allowed hydrates to form at much milder thermodynamic conditions than those required for the production of pure methane hydrates. Moreover, the addition of propane strengthened the hydrate lattice, ensuring its stability also at temperatures unsuitable for the permanence of pure propane hydrates. The same criterion was used for the third mixture, where the concentration of ethane was calculated according to Gambelli et al., (2025) [40]. The concentrations of each mixture were finally modified in order to include the target quantity of hydrogen. In detail, the second mixture containing propane substantially consists of the first mixture with a slightly increased quantity of hydrogen and was studied to verify whether an excess of this latter species would enhance or negatively affect the overall energy stored per unit volume of hydrate.

This study is not focused on maximizing the quantity of gas captured into hydrates; rather, the research aims to determine how much hydrogen can be captured into hydrates when mixed with the selected support gases; moreover, this study also aims to quantify the maximum energy theoretically stored in hydrates, as a function of the selected mixture. For that reason, chemical promoters were not considered and only the composition of the gaseous phase captured into hydrates was measured and discussed in this section.

Each gas composition measurement was carried out in triplicate. The value measured, together with the related uncertainties, is indicated in Table 2, while an example of chromatographic analysis carried out to define the values reported in Table 2 is graphically shown in Figure 4.

Table 2. Composition of the gas phase captured into hydrates for each mixture and related uncertainty.

Mixture 1		Mixture 2		Mixture 3	
H_2	16.21 ± 0.01 [vol%]	H_2	38.48 ± 0.01 [vol%]	H_2	34.69 ± 0.01 [vol%]
CH_4	83.74 ± 0.01 [vol%]	CH_4	61.46 ± 0.01 [vol%]	CH_4	20.00 ± 0.01 [vol%]
C_3H_8	0.04 ± 0.01 [vol%]	C_3H_8	0.05 ± 0.01 [vol%]	C_2H_6	45.31 ± 0.01 [vol%]

The first concept to highlight is the relatively elevated hydrogen capture observed, regardless of the typology of mixture used. According to gas-chromatographic analyses the concentration of hydrogen in the gas phase captured into hydrates ranged from 16.21 vol% (Mixture 1) to 38.48 vol% (Mixture 2). The adoption of ternary mixtures is responsible for that positive result: the two support species stabilized both the small and the large cavities

of the hydrate lattice, thus allowing hydrogen molecules to occupy the vacant cavities and, at the same time, ensuring the required stability.

The mixtures containing propane showed an increase in hydrogen captured in hydrates as a function of the initial concentration of hydrogen in the gas mixture. In detail, the difference between the two values is significant, namely 16.21 vol% for Mixture 1, initially containing 30 vol% H_2, and 38.48 vol% for Mixture 2, initially containing 40 vol% H_2. Such a difference highlighted the great stability provided to the crystalline lattice by the support gases, as well as the large availability of free cages. Therefore, the larger the abundance of hydrogen molecules, the higher the capture of those molecules. This trend can be easily explained in terms of hydration number, or the ratio between water and gas molecules in the hydrate lattice. For sI hydrates, as a function of the cage occupancy, it could range from 5.75 to 19, confirming the large availability of free cavities, if the overall crystalline structure is stable enough [3]. However, it should be noted that experiments carried out in this study do not provide quantitative information about the mole of hydrates formed and the corresponding quantity of gas captured; only qualitative indications about the concentrations of each species which can be theoretically reached are provided in this study.

The gas analyses also revealed that propane did not directly participate in the formation of hydrates: its concentration did not exceed 0.05 vol%, even if its contribution to the formation process clearly appeared.

A similar phenomenon was already observed and documented in the literature. In Gambelli et al., (2023) [59] replacement tests were carried out with a mixture of CO_2/C_3H_8 (90/10) vol%. The presence of propane enhanced the replacement of methane and increased the overall quantity of hydrates present in the reactor after replacement (the total quantity of hydrates increased from 0.083 mol to 0.145 mol). Moreover, the molar fractions of, respectively, methane, carbon dioxide and propane in hydrates were equal to 0.154, 0.788 and 0.058 mf, meaning that the quantity of methane recovered exceeded 75% of the maximum quantity theoretically recoverable when replacement is carried out with pure carbon dioxide. Even if minimally involved in the formation of hydrates, propane favored the capture of carbon dioxide.

As a conclusion, when $H_2/CH_4/C_3H_8$ mixtures were used, the final concentration of hydrogen slightly decreased and the opposite occurred for methane, while the concentration of propane, found in hydrates, can be considered negligible.

The trend radically changed when ethane was used instead of propane (Mixture 3). The concentration of hydrogen in hydrates was higher than its initial presence in the gas mixture (34.69 vol% against 30 vol%), while the concentration of methane dropped from 52 vol% to 20 vol%. Unlike propane, a large amount of ethane was captured into hydrates: the analyses of the gas composition within the crystalline lattice revealed the presence of 45.31 vol% C_2H_6. Such a different result can be explained in terms of capability of the various species to form sI hydrates. While propane cannot occupy the cages forming sI hydrate, ethane molecules can fit and effectively stabilize the large $5^{12}6^2$ cavities of sI. Since this structure contains 75% of large cavities, the inclusion of ethane provided great stability to the system and the capture of hydrogen was consequently facilitated. Therefore, the hydrate formation process acted as a hydrogen concentrator in this latter case, being the concentration of this species in hydrates higher than its initial value in Mixture 3.

Table 3 shows the concentrations previously discussed, expressed as percentage by weight (wt%) and allows to compare the present storage solution with the traditional techniques, widely documented in literature. The table shows the maximum quantity of each gas which can be stored in one cubic meter of hydrates. In detail, the values were calculated by considering 100% cage occupancy. Considering the typology of hydrate formed and, mostly, the guest species involved in the process, such an ideal maximum

value may significantly vary [60]. When hydrates are carried out with pure hydrogen, one cubic meter of crystalline lattice may contain up to 478 Nm^3 of hydrogen while, when pure methane is considered, the same theoretical value is equal to 172 Nm^3 [38,47,60,61]. Considering the quantity of methane captured and willing to provide a precautionary estimation, the lowest value (172 Nm^3_{GAS}/m^3_{HYD}) was considered. According to this and based on the molar fraction of each species, the overall weight of the gas phase contained in one cubic meter of hydrates was equal to 2.36 kg for Mixture 1, 1.84 kg for Mixture 2 and 3.01 kg for Mixture 3. The table shows, for each species, the quantity, in grams, included in one cubic meter of hydrates and the corresponding percentage by weight.

Table 3. Quantity of each species contained in one cubic meter of hydrates, calculated assuming 172 Nm^3_{GAS}/m^3_{HYD}, corresponding to a theoretical 100% cage occupancy, and the corresponding percentage by weight.

Species	Mixture 1		Mixture 2		Mixture 3	
	g/m^3_{HYD}	wt%	g/m^3_{HYD}	wt%	g/m^3_{HYD}	wt%
H_2	55.8	2.36	132.4	7.25	119.3	3.97
CH_4	2304.5	97.51	1691.4	92.53	550.4	18.3
C_2H_6	---	---	---	---	2338.0	77.73
C_3H_8	3.0	0.13	3.8	0.22	---	---

The concentration of hydrogen ranged from 2.36 to 7.25 wt%. According to the data available in the literature, these values are compatible with other hydrogen storage technologies, such as Metal Organic Frameworks (MOFs) and Metal Hydrides (MHs) [62]. For each species, the concentrations in volume (vol%) and by weight (wt%), as a function of the initial mixture tested, are graphically shown in Figures 5 and 6.

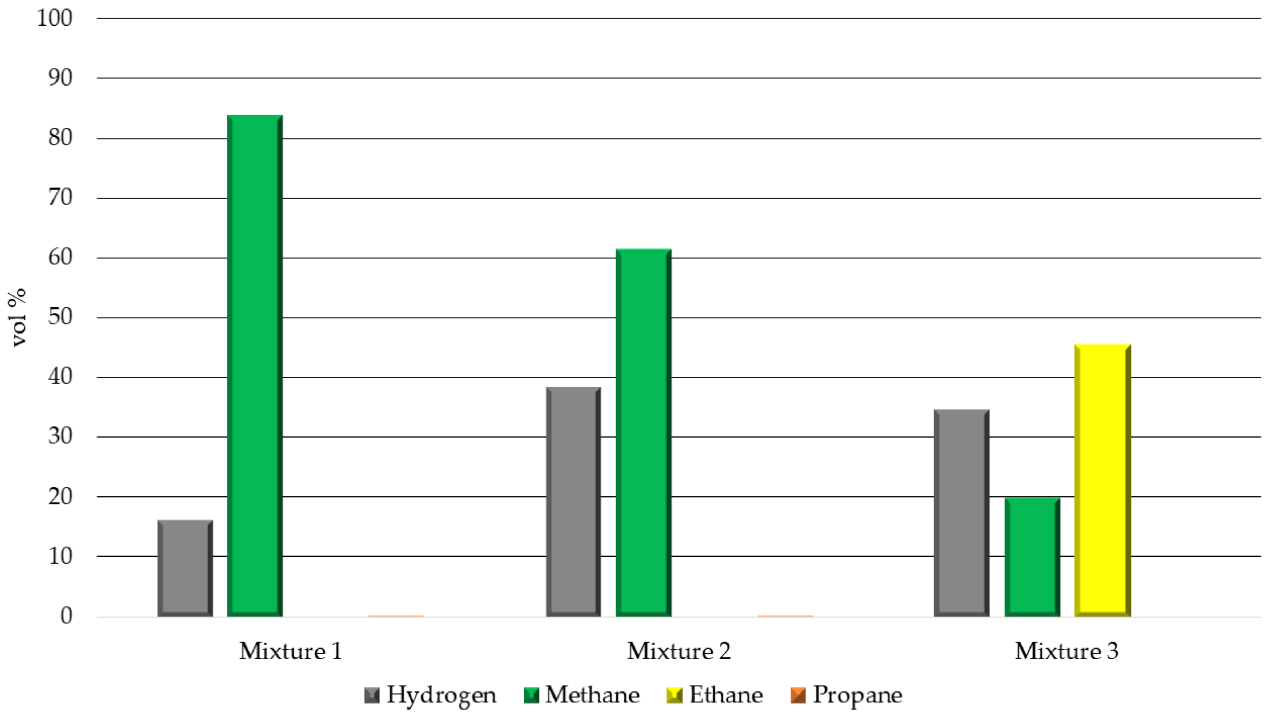


Figure 5. Concentrations in volume (vol%) for each species in the hydrate phase, as a function of the initial mixture tested.

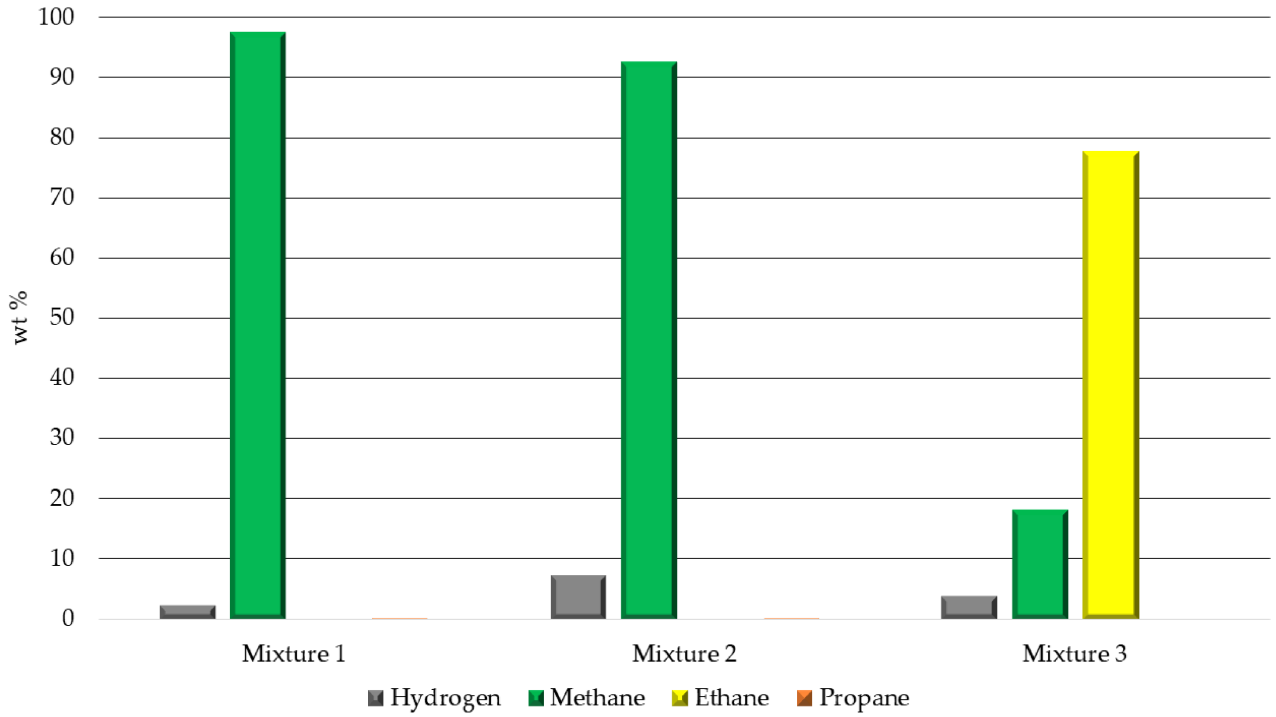


Figure 6. Concentrations by weight (wt%) for each species in the hydrate phase, as a function of the initial mixture tested.

The results also showed a good consistency with the current literature: according to Strobel and colleagues [63], when stored in hydrates, the concentration of hydrogen could vary from 4.0 to 5.6 wt%, also depending on the process kinetics [64]. However, it should be noted that most studies on hydrogen capture in hydrates were carried out by using appropriate chemical promoters, which were not considered in the present research.

The use of ethane, instead of propane, widely changed the gas composition captured into hydrates. The difference does not fall on the quantity of hydrogen captured, but it is visible on the support gas captured together with hydrogen. In mixtures involving propane (Mixture 1 and Mixture 2), the quantity of methane captured into hydrates was extremely high and varied from 92.53 to 97.51 vol%, whereas it dropped to 18.3 wt% in the presence of ethane (Mixture 3). This trend further confirms the formation of sI hydrates and the higher stability of the system when ethane molecules are involved, due to the stabilization of the large $5^{12}6^2$ cavities.

According to the concentrations of each species, the following energy evaluations were provided:

- The lower heating value of the gas mixture captured into hydrates [MJ/kg] (Table 4);
- The energy [MJ] of each species, related to one cubic meter of hydrates (see Table 5 and Figure 7);
- The overall energy contained in one cubic meter of hydrates [MJ/m^3_{HYD}] (see Table 4 and Figure 7).

Table 4. Lower heating value (LHV) of the gas mixtures captured into hydrates and overall energy contained (E) in one cubic meter of hydrate (considering 100% cage occupancy).

	LHV [MJ/kg]	kg/m^3_{HYD}	E [MJ/m^3_{HYD}]
Mixture 1	51.65	2.36	122.1
Mixture 2	55.07	1.83	100.6
Mixture 3	51.12	3.01	153.7

Table 5. Energy, corresponding to each species, stored in one cubic meter of hydrate (considering 100% cage occupancy).

Species	Mixture 1 [MJ]	Mixture 2 [MJ]	Mixture 3 [MJ]
H_2	6.7	15.9	14.3
CH_4	115.2	84.6	27.5
C_2H_6	---	---	111.8
C_3H_8	0.2	0.2	---

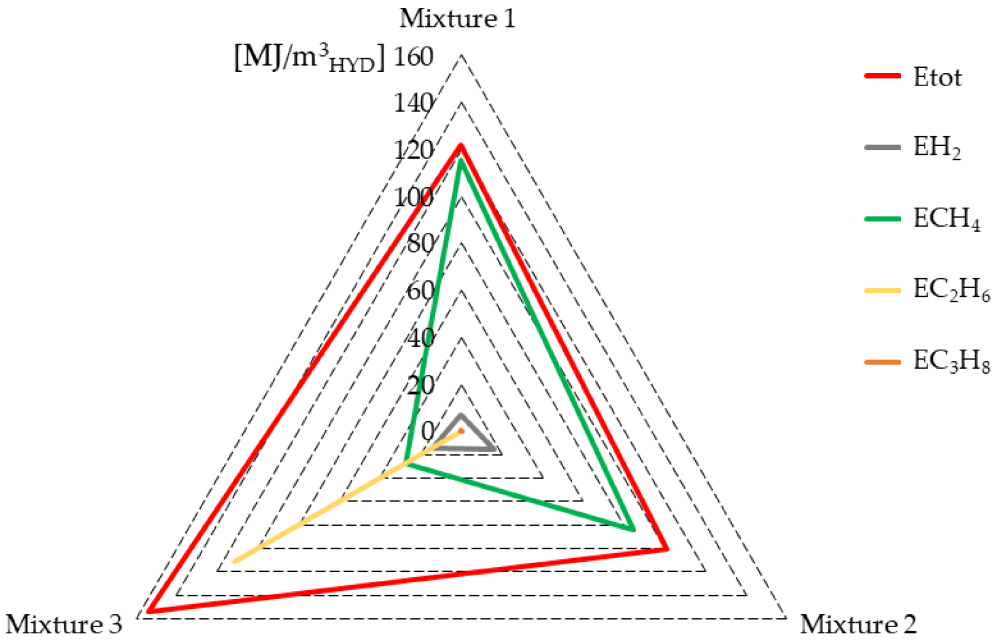


Figure 7. Overall energy contained in one cubic meter of hydrates and quantity of energy corresponding to each specific guest species.

The three mixtures found in hydrates assumed similar LHV, which ranged from 51.12 to 55.07 MJ/kg. The highest value was obtained with the sample corresponding to Mixture 2, or the one showing the highest concentration of hydrogen (wt%) and the positive difference can be therefore attributed to this latter species.

Conversely, a marked difference exists between the total quantity of energy (related to one cubic meter of hydrates and assuming 100% cage occupancy) calculated for each sample. Here, the best result was obtained with the ethane-containing mixture (Mixture 3), with 153.7 MJ/m^3_{HYD}. However, the difference observed with the values corresponding to the other mixtures, is mainly a function of the massive inclusion of ethane and cannot be attributed to hydrogen.

Regarding the quantity of energy stored related to the sole hydrogen, the most attractive results correspond to Mixture 2, whose capture in hydrates allowed to store 15.9 MJ/m^3_{HYD} in the form of hydrogen, and to Mixture 3, where 14.3 MJ/m^3_{HYD} were stored via hydrogen capture.

A comparison with hydrogen storage systems reported in the recent literature is presented in Table 6. The hydrogen storage capacities estimated in the present work ranged from 2.36 wt% to 7.25 wt%, depending on the gas mixture adopted. These values are comparable with those reported for several hydrogen–hydrate storage systems, Metal–Organic Frameworks (MOFs) and Mg-based metal hydrides.

Table 6. Comparison of gravimetric hydrogen storage capacities reported in the literature and estimated in the present study.

Technology	H_2 Storage Capacity (wt%)	Data Type	Ref.
Confined hydrogen hydrates	4.1–5.0	Experimental	[65]
Promoted hydrates	3.2–4.25	Calculated	[66]
2D hydrogen hydrates	0.30–1.01	Calculated	[67]
Nano-confined hydrates	~3.2	Experimental	[68]
MOFs	1.5–7.0	Review	[69]
Mg-based hydrides	6.0–7.6	Review and Experimental	[70,71]
Present work	2.36–7.25	Calculated	This work

Recent studies have demonstrated that the hydrogen storage capacity of hydrate-based systems strongly depends on the adopted promotion strategy. For instance, Mi et al. [66] reported theoretical storage capacities between 0.30 and 1.01 wt% for promoter-assisted hydrogen hydrates, highlighting the trade-off between improved formation conditions and hydrogen uptake. Similarly, Liu et al. [67] showed that confinement effects can significantly enhance storage performance, with theoretical capacities ranging from 3.20 to 4.25 wt% for two-dimensional hydrogen hydrate structures. Along the same line, Farrando-Perez et al. [66] experimentally demonstrated that hydrogen clathrates confined within activated carbon materials may reach capacities up to 5.0 wt%, while Ciocarlan et al. [68] proposed nano-confined hydrate systems in mesoporous silica with theoretical capacities close to 3.2 wt%.

Comparable storage capacities have also been reported for alternative hydrogen storage technologies. Sutton et al. [69] observed that the gravimetric capacity of MOFs may vary from approximately 1.5 to 7.0 wt%, depending on the material characteristics and operating conditions. Regarding metal hydrides, Nivedhitha et al. [70] reported storage capacities ranging from 6.0 to 7.6 wt% for Mg-based materials, while Zhang et al. [71] demonstrated that optimized ultrafine MgH_2 nanoparticles can achieve reversible hydrogen storage capacities of approximately 6.7 wt%.

The highest hydrogen storage capacity estimated in the present study (7.25 wt%, Mixture 2) therefore falls within the upper range reported for several advanced hydrogen storage materials. However, it should be emphasized that the capacities reported herein were derived from experimentally measured gas compositions within the hydrate phase and subsequently converted into gravimetric capacities assuming ideal hydrate cage occupancy. Consequently, the reported values represent theoretical storage capacities associated with the gas composition captured within the hydrate lattice rather than experimentally measured capacities of the complete storage system. Therefore, the comparison with MOFs and metal hydrides should be interpreted as a qualitative benchmark intended to position the proposed hydrate-based storage approach within the broader hydrogen storage landscape.

6. Conclusions

This research deals with hydrates with ternary H_2-containing gaseous mixtures, aiming at enhancing the capture of hydrogen. When used in pure form, hydrogen requires extremely severe thermodynamic conditions to be captured and the process is feasible exclusively via the use of chemical promoters.

Three mixtures were tested: $H_2/CH_4/C_3H_8$ (30/60/10) and (40/50/10) vol% and $H_2/CH_4/C_2H_6$ (30/52/18) vol%. Hydrates were formed in excess of gas and samples of the mixtures captured into hydrates were withdrawn and analyzed via gas-chromatographic analysis. The results showed high capture of hydrogen, whose concentration in the hydrate phase ranged from 16.21 to 38.48 vol%, even if the forming conditions were much milder than those required for the production of pure hydrogen hydrates (in this study: temperatures above 0 °C and pressures lower than 55 bar). Considering the composition of each component, the lower heating values of mixtures captured into hydrates were equal to 51.12–55.07 MJ/mol. Assuming 100% ideal cage occupancy, the total quantity of energy captured in one cubic meter of hydrates varies from 100.6 MJ to 153.7 MJ, proving the high energy density theoretically achievable in hydrates. The quantity of energy stored in a unit volume of hydrates in the form of hydrogen was equal to 6.7–15.9 MJ.

This study proved that the selected support gases provided enough stability to the crystalline lattice to allow hydrogen molecules to occupy the vacant cavities. Future studies will be devoted to maximizing the production of hydrates with the ternary mixtures, proposed and tested in the present research, in order to fully validate the proposed method as an alternative hydrogen-storage solution and, possibly, to test the proposed solution on a larger scale.

Author Contributions: Conceptualization, A.M.G.; methodology, A.M.G., F.F. and L.B.; software, F.F.; validation, A.D.G. and F.R.; formal analysis, A.M.G. and L.B.; investigation, A.M.G. and F.F.; resources, F.F. and F.R.; data curation, A.M.G. and A.D.G.; writing—original draft preparation, A.M.G. and L.B.; project administration, F.R.; funding acquisition, F.F. and F.R. All authors have read and agreed to the published version of the manuscript.

Funding: The authors gratefully acknowledge financial support derived by the PNRR project (Missione 2 "Rivoluzione verde e transizione ecologica", Componente 2 "Energia rinnovabile, idrogeno, rete e mobilità sostenibile", Investimento 3.5 "Ricerca e sviluppo sull'idrogeno", Finanziato dall'Unione Europea–Next Generation EU a valere sul decreto del Ministro della Transizione Ecologica del 23 December 2021, n. 545 articolo 1, comma 5, lettera B.) entitled: "High Efficiency Hydrogen Storage (HEHS)", ID: RSH2B_000052.

Data Availability Statement: Data are already included in the text. More experimental details will be available upon request to the corresponding author.

Acknowledgments: The authors also acknowledge the technical and material contribution of AiZoOn Technology Consulting and Nippon Gases Industrial S.r.l.

Conflicts of Interest: Author Fabiano Ferrari was employed by the company Nippon Sanso Industrial S.r.l. (formerly Nippon Gases Industrial S.r.l.). The remaining authors declare that the research was conducted in the absence of any commercial or financial relationships that could be construed as a potential conflict of interest.

References

1. Siazik, J.; Malcho, M.; Lenhard, R. Proposal of experimental device for the continuous accumulation of primary energy in natural gas hydrates. *EPJ Web Conf.* **2017**, *143*, 02106. [CrossRef]
2. Loveday, J.S.; Nelmes, R.J. High-pressure gas hydrates. *Phys. Chem. Chem. Phys.* **2008**, *10*, 937–950. [PubMed]
3. Sloan, E.D.; Koh, C.A. *Clathrate Hydrates of Natural Gases*, 3rd ed.; Taylor & Francis Group, CRC Press: Boca Raton, FL, USA, 2008.
4. Hassanpouryouzband, A.; Yang, J.; Tohidi, B.; Chuvilin, E.; Istomin, V.; Bukhanov, B.; Cheremisin, A. CO_2 capture by injection of flue-gas or CO_2-N_2 mixtures into hydrate reservoirs: Dependence of CO_2 capture efficiency on gas hydrate reservoir conditions. *Environ. Sci. Technol.* **2018**, *52*, 4324–4330. [PubMed]
5. Gambelli, A.M.; Filipponi, M.; Nicolini, A.; Rossi, F. Natural gas hydrate: Effect of sodium chloride on the CO_2 replacement process. *Int. Multidiscip. Sci. GeoConf. SGEM* **2019**, *4*, 333–343.
6. Jahangiri, S.; Varaminian, F. Determination of the intrinsic kinetic rate constant of carbon dioxide hydrate formation. *J. Mol. Liq.* **2025**, *438*, 128559. [CrossRef]

7. Hou, X.; Sun, Z. Effect of Thiazolidine as thermodynamic inhibitor on hydrate phase equilibrium conditions of carbon dioxide. *J. Chem. Thermodyn.* **2026**, *212*, 107582.
8. Sun, H.; Chen, J.; Karunakaran, G.; Chen, B. System-level insights into flow-pressure-saturation coupling for safe and efficient methane hydrate production. *Appl. Energy* **2026**, *411*, 127623.
9. Hoshikawa, A.; Hachikubo, A. Observation of hydrogen bonding network in hydrogen sulfide hydrate using neutron diffraction. *Chem. Phys. Let.* **2023**, *812*, 140274.
10. Xiao, Y.; Li, A.R.; Wu, J.; Li, B.; Yao, H. Thermodynamic modelling for ternary clathrate hydrates of carbon dioxide, nitrogen and tetrahydrofuran. *J. Chem. Thermodyn.* **2023**, *184*, 107091. [CrossRef]
11. Makogon, Y.F. *Hydrates of Natural Gas*; PennWell: Tulsa, OK, USA, 1981.
12. Jeffrey, G.A. Hydrate inclusion compounds. *J. Incl. Phenom.* **1984**, *1*, 211–222. [CrossRef]
13. Pauling, L.; Marsh, R.E. The structure of chlorine hydrate. *Proc. Natl. Acad. Sci. USA* **1952**, *38*, 112–118. [CrossRef] [PubMed]
14. Cui, J.; Sun, Z.; Wang, X.; Yu, B.; Leng, S.; Chen, G.; Sun, C. Fundamental mechanisms and phenomena of clathrate hydrate nucleation. *Chin. J. Chem. Eng.* **2019**, *27*, 2014–2025. [CrossRef]
15. Claussen, W.F. A second water structure for inert gas hydrates. *J. Chem. Phys.* **1951**, *19*, 1425–1426. [CrossRef]
16. Ripmeester, J.A.; Tse, J.S.; Ratcliffe, C.I.; Powell, B.M. A new clathrate hydrate structure. *Nature* **1987**, *325*, 135–136. [CrossRef]
17. Wang, T.; Sun, L.; Fan, Z.; Wei, R.; Li, Q.; Yao, H.; Dong, H.; Zhang, L.; Yang, L.; Zhao, J.; et al. Promoting CH_4/CO_2 replacement from hydrate with warm brine injection for synergistic energy harvest and carbon sequestration. *Chem. Eng. J.* **2023**, *457*, 141129.
18. Gambelli, A.M.; Presciutti, A.; Rossi, F. Kinetic considerations and formation rate for carbon dioxide hydrate, formed in presence of a natural silica-based porous medium: How initial thermodynamic conditions may modify the process kinetic. *Thermochim. Acta* **2021**, *705*, 179039. [CrossRef]
19. Cao, X.; Wang, H.; Yank, K.; Wu, S.; Chen, Q.; Bian, J. Hydrate-based CO_2 sequestration technology: Feasibilities, mechanisms, influencing factors, and applications. *J. Pet. Sci. Eng.* **2022**, *219*, 111121. [CrossRef]
20. Aminu, M.D.; Nabavi, S.; Rochelle, C.; Manovìc, V. A review of developments in carbon dioxide storage. *Appl. Energy* **2017**, *208*, 1389–1419. [CrossRef]
21. Dyadin, Y.A.; Larionov, E.G.; Manakov, A.Y.; Zhurko, F.V.; Aladko, E.Y.; Mikina, T.V.; Komarov, V.Y. Clathrate hydrates of hydrogen and neon. *Mendeleev Commun.* **1999**, *9*, 209–210. [CrossRef]
22. Smirnov, G.S.; Stegailov, V.V. Toward determination of the new hydrogen hydrate clathrate structures. *J. Phys. Chem. Lett.* **2013**, *4*, 3560–3564. [CrossRef]
23. Zhang, L.; Dong, H.; Dai, S.; Kuang, Y.; Yang, L.; Wang, J.; Zhao, J.; Song, Y. Effects on depressurization on gas production and water performance from excess-gas and excess-water methane hydrate accumulations. *Chem. Eng. J.* **2022**, *431*, 133223.
24. Montazeri, S.M.; Kolliopoulos, G. Hydrate based desalination for sustainable water treatment: A review. *Desalination* **2022**, *537*, 115855. [CrossRef]
25. Gaikward, N.; Nakka, R.; Khavala, V.; Bhadani, A.; Mamane, H.; Kumar, R. Gas hydrate-based process for desalination of heavy metal ions from an aqueous solution: Kinetics and rate of recovery. *ACS ES T Water* **2021**, *1*, 134–144.
26. Claben, T.; Seidl, P.; Loekman, S.; Gatternig, B.; Rauch, C.; Delgado, A. Review on the food technological potentials for gas hydrate technology. *Curr. Opin. Food. Sci.* **2019**, *29*, 48–55. [CrossRef]
27. Srivastava, S.; Hitzmann, B.; Zettel, V. A future road map for carbon dioxide (CO_2) gas hydrate as an emerging technology in food research. *Food Bioprocess Technol.* **2021**, *14*, 1758–1762. [CrossRef]
28. Wang, F.; Guo, G.; Liu, G.Q.; Luo, S.J.; Guo, R.B. Effects of surfactants micelles and surfactant-coated nanospheres on methane hydrate growth pattern. *Chem. Eng. Sci.* **2016**, *144*, 108–115. [CrossRef]
29. Hua, T.Q.; Ahluwalia, R.K.; Peng, J.K.; Kromer, M.; Lasher, S.; McKenney, K.; Law, K.; Sinha, J. Technical assessment compressed hydrogen storage tank systems for automotive applications. *Int. J. Hydrogen Energy* **2011**, *36*, 3037–3049. [CrossRef]
30. Yanxing, Z.; Maoqiong, G.; Yuan, Z.; Xueqiang, D.; Jun, S. Thermodynamics analysis of hydrogen storage based on compressed gaseous hydrogen, liquid hydrogen and cryo-compressed hydrogen. *Int. J. Hydrogen Energy* **2019**, *22*, 16833–16840. [CrossRef]
31. Sethia, G.; Sayari, A. Activated carbon with optimum pore size distribution for hydrogen storage. *Carbon* **2016**, *99*, 289–294. [CrossRef]
32. Li, G.; Kobayashi, H.; Taylor, J.M.; Ikeda, R.; Kubota, Y.; Kato, K.; Takata, M.; Yamamoto, T.; Toh, S.; Matsumura, S.; et al. Hydrogen storage in Pd nanocrystals covered with a metal organic framework. *Nat. Mater.* **2014**, *13*, 802–806. [CrossRef] [PubMed]
33. Jorgensen, S.W. Hydrogen storage tanks for vehicles: Recent progress and current status. *Curr. Opin. Solid State Mater. Sci.* **2011**, *15*, 39–43. [CrossRef]
34. Zohuri, B. Cryogenics and liquid hydrogen storage. In *Hydrogen Energy*; Springer: Cham, Switzerland, 2019; pp. 121–139.
35. Stamatakis, E.; Zoulias, E.; Tzamalis, G.; Massina, Z.; Analytis, V.; Christodoulou, C.; Stubos, A. Metal hydride hydrogen compressors: Current developments and early markets. *Renew. Energy* **2018**, *127*, 850–862. [CrossRef]

36. Hashimoto, S.; Sugahara, T.; Moritoki, M.; Sato, H.; Ohgaki, K. Thermodynamic stability of hydrogen + tetra-n-butyl ammonium bromide mixed gas hydrate in nonstoichiometric aqueous solutions. *Chem. Eng. Sci.* **2008**, *63*, 1092–1097.
37. Du, J.; Wang, L.; Liang, D.; Li, D. Phase equilibria and dissociation enthalpies of hydrogen semi-clathrate hydrate with tetrabutyl ammonium nitrate. *J. Chem. Eng. Data* **2021**, *57*, 603–609.
38. Zhang, Y.; Bhattacharjee, G.; Kumar, R.; Linga, P. Solidified hydrogen storage (Solid-HyStore) via clathrate hydrates. *Chem. Eng. J.* **2022**, *431*, 133702.
39. Gambelli, A.M. Hydrates production with gaseous CO_2/C_3H_8 and CH_4/C_3H_8 (90/10 vol%) mixtures and definition of the role of propane during CO_2/CH_4 replacement processes. *J. CO_2 Util.* **2024**, *88*, 102936.
40. Gambelli, A.M.; Rossi, F.; Gigliotti, G. Formation and melting of hydrate with binary CO_2/C_2H_6 mixtures in silica sand: Comparison between dissociation data and phase equilibrium of pure CO_2 and C_2H_6 hydrates. *C* **2025**, *11*, 63.
41. Barelli, L.; Bidini, G.; Ottaviano, A. Hydromethane generation through SOE (solid oxide electrolyser): Advantages of H_2O-CO_2 co-electrolysis. *Energy* **2015**, *90*, 1180–1191.
42. Villante, C.; Genovese, A. Hydromethane: A bridge towards the hydrogen economy or an unsustainable promise? *Int. J. Hydrogen Energy* **2012**, *37*, 11541–11548. [CrossRef]
43. Gambelli, A.M.; Pezzolla, D.; Rossi, F.; Gigliotti, G. Hydrates formed with binary CH_4/C_2H_6 mixtures: Effects of adding 25–75 vol% ethane on the quantity of hydrates formed, growth mechanism and structure preservation. *C* **2025**, *11*, 88.
44. Bu, F.; Wang, Z.; Wajid, A.; Zhai, R.; Liu, T.; Li, Y.; Ji, X.; Liu, X.; Ding, S.; Cheng, Y.; et al. Solid–State Hydrogen Storage Materials with Excellent Selective Hydrogen Adsorption in the Presence of Alkanes, Oxygen, and Carbon Dioxide by Atomic Layer Amorphous Al_2O_3 Encapsulation. *Nanomicro Lett.* **2026**, *18*, 78. [CrossRef] [PubMed]
45. Lim, K.L.; Kazemian, H.; Yaakob, Z.; Daud, W.R.W. Solid-state Materials and Methods for Hydrogen Storage: A Critical Review. *Chem. Eng. Technol.* **2010**, *33*, 213–226. [CrossRef]
46. Englezos, P.; Lee, J.D. Gas Hydrates: A Cleaner Source of Energy and Opportunity for Innovative Technologies. *Korean J. Chem. Eng.* **2005**, *22*, 671–681. [CrossRef]
47. Lang, X.; Fan, S.; Wang, Y. Intensification of Methane and Hydrogen Storage in Clathrate Hydrate and Future Prospect. *J. Nat. Gas Chem.* **2010**, *19*, 203–209. [CrossRef]
48. Rothmund, E.V.; He, J.; Zhang, Z.; Xiao, S. Promoting Hydrogen Storage Under Mild Conditions by Binary Clathrate Hydrates in Porous Activated Carbon. *Chem. Eng. J.* **2025**, *521*, 166696. [CrossRef]
49. Lee, H.; Seo, Y.; Seo, Y.; Moudrakovski, I.L.; Ripmeester, J.A. Recovering Methane from Solid Methane Hydrate with Carbon Dioxide. *Angew. Chem. Int. Ed.* **2003**, *42*, 5048–5051. [CrossRef] [PubMed]
50. Chaturvedi, K.R.; Sharma, T.; Trivedi, J.; Kumar, G.S. Experimental Investigation for Comparative Effectiveness of CO_2+N_2 and CO_2+N_2+H_2 on Integrated Methane Production and Carbon Storage from Natural Hydrate Media. *J. Environ. Chem. Eng.* **2023**, *11*, 109388. [CrossRef]
51. Sun, Y.-F.; Wang, Y.-F.; Zhong, J.-R.; Li, W.-Z.; Li, R.; Cao, B.-J.; Kan, J.-Y.; Sun, C.-Y.; Chen, G.-J. Gas Hydrate Exploitation Using CO_2/H_2 Mixture Gas by Semi-Continuous Injection-Production Mode. *Appl. Energy* **2019**, *240*, 215–225. [CrossRef]
52. Sun, Y.-F.; Zhong, J.-R.; Li, R.; Zhu, T.; Cao, X.-Y.; Chen, G.-J.; Wang, X.-H.; Yang, L.-Y.; Sun, C.-Y. Natural Gas Hydrate Exploitation by CO_2/H_2 Continuous Injection-Production Mode. *Appl. Energy* **2018**, *226*, 10–21. [CrossRef]
53. Wang, X.-H.; Sun, Y.-F.; Wang, Y.-F.; Li, N.; Sun, C.-Y.; Chen, G.-J.; Liu, B.; Yang, L.-Y. Gas Production from Hydrates by CH_4-CO_2/H_2 Replacement. *Appl. Energy* **2017**, *188*, 305–314. [CrossRef]
54. Trippetta, F.; Gambelli, A.M.; Minelli, G.; Castellani, B.; Rossi, F. Sustainability of CO_2 replacement processes in marine hydrate reservoirs: Factors causing changes on mechanical properties of gas-hydrate after CO_2/CH_4 exchange. *Proc. Saf. Environ. Prot.* **2023**, *179*, 628–639. [CrossRef]
55. Gambelli, A.M.; Rossi, F. Experimental characterization of the difference in induction period between CH_4 and CO_2 hydrates: Motivations and possible consequences on the replacement process. *J. Nat. Gas Sci. Eng.* **2022**, *108*, 104848. [CrossRef]
56. Gambelli, A.M. Methane replacement into hydrate reservoirs with carbon dioxide: Main limiting factors and influence of the gaseous phase composition, over hydrates, on the process. *Chem. Eng. J.* **2023**, *478*, 147247. [CrossRef]
57. Wilson, P.W.; Haymet, A.D.J. Hydrate formation and re-formation in nucleating THF/water mixtures show no evidence to support a "memory" effect. *Chem. Eng. J.* **2010**, *161*, 146–150.
58. Ripmeester, J.A.; Alavi, S. Some current challenges in clathrate hydrate science: Nucleation, decomposition and the memory effect. *Curr. Opin. Solid State Mater. Sci.* **2016**, *20*, 344–351. [CrossRef]
59. Gambelli, A.M.; Rossi, F.; Gigliotti, G. Methane replacement by using CO_2/C_3H_8 mixtures for carbon storage and enhanced methane recovery in gas hydrates. *Gas Sci. Eng.* **2023**, *115*, 205028.
60. Lan, X.; Chen, J.; Li, D.; Zheng, J.; Linga, P. Gas storage via clathrate hydrates: Advances, challenges, and prospects. *Gas Sci. Eng.* **2024**, *129*, 205388. [CrossRef]
61. Veluswamy, H.P.; Kumar, A.; Seo, Y.; Lee, J.D.; Linga, P. A review of solidified natural gas (SNG) technology for gas storage via clathrate hydrates. *Appl. Energy* **2018**, *216*, 262–285. [CrossRef]

62. Di Profio, P.; Arca, S.; Rossi, F.; Filipponi, M. Comparison of hydrogen hydrates with existing hydrogen storage technologies: Energetic and economic evaluations. *Int. J. Hydrogen Energy* **2009**, *34*, 9173–9180. [CrossRef]
63. Strobel, T.A.; Koh, C.A.; Sloan, E.D. Water cavities of sH clathrate hydrate stabilized by molecular hydrogen. *J. Phys. Chem. B Lett.* **2008**, *112*, 1885–1887. [CrossRef]
64. Lee, H.; Lee, J.; Kim, D.Y.; Park, J.; Seo, Y.T.; Zeng, H.; Moudrakovsky, I.L.; Ratcliffe, C.I.; Ripmeester, J.A. Tuning clathrate hydrates for hydrogen storage. *Nature* **2005**, *434*, 743–746. [CrossRef] [PubMed]
65. Farrando-Perez, J.; Balderas-Xicohtencatl, R.; Cheng, Y.; Daemen, L.; Cuadrado-Collados, C.; Martinez-Escandell, M.; Ramirez-Cuesta, A.J.; Silvestre-Albero, J. Rapid and efficient hydrogen clathrate hydrate formation in confined nanospace. *Nat. Commun.* **2022**, *13*, 5953. [CrossRef] [PubMed]
66. Mi, F.; Ning, F.; Vlugt, T.J.H.; Moultos, O.A. Molecular insight into hydrogen storage in clathrate hydrates: The effect of different promoters on the spontaneous nucleation of hydrogen hydrates studied via microsecond-scale molecular dynamics simulations. *Chem. Eng. J.* **2025**, *512*, 162253. [CrossRef]
67. Liu, J.; Wang, J.; Yuan, Y.; Chi, F.; Liu, S. Hydrogen storage properties of two-dimensional clathrate hydrates: A theoretical study. *Chem. Phys. Lett.* **2024**, *851*, 141499. [CrossRef]
68. Ciocarlan, R.-G.; Farrando-Perez, J.; Arenas-Esteban, D.; Houlleberghs, M.; Daemen, L.L.; Cheng, Y.; Ramirez-Cuesta, A.J.; Breynaert, E.; Martens, J.; Bals, S.; et al. Tuneable mesoporous silica material for hydrogen storage application via nano-confined clathrate hydrate construction. *Nat. Commun.* **2024**, *15*, 8697. [CrossRef] [PubMed]
69. Sutton, A.L.; Mardel, J.I.; Hill, M.R. Metal-Organic Frameworks (MOFs) as Hydrogen Storage Materials at Near-Ambient Temperature. *Chem. Eur. J.* **2024**, *30*, e202400717. [PubMed]
70. Nivedhitha, S.; Sankar, K.V.; Praveen Kumar, S.; Kalai Selvan, R. Recent advances in Mg-based materials for hydrogen storage applications: A review. *Sustain. Energy Fuels* **2025**, *9*, 5061–5100.
71. Zhang, X.; Liu, Y.; Ren, Z.; Zhang, X.; Hu, J.; Huang, Z.; Lu, Y.; Gao, M.; Pan, H. Realizing 6.7 wt% reversible storage of hydrogen at ambient temperature with non-confined ultrafine magnesium hydrides. *Energy Environ. Sci.* **2021**, *14*, 2302–2313.

Disclaimer/Publisher's Note: The statements, opinions and data contained in all publications are solely those of the individual author(s) and contributor(s) and not of MDPI and/or the editor(s). MDPI and/or the editor(s) disclaim responsibility for any injury to people or property resulting from any ideas, methods, instructions or products referred to in the content.